

Validation of Comprehensive Helicopter Aeroelastic Analysis with Experimental Data

Shrinivas R. Bhat and Ranjan Ganguli
Indian Institute of Science, Bangalore-560 012

ABSTRACT

The experimental data for a 4-bladed soft-inplane hingeless main rotor is used to validate a comprehensive aeroelastic analysis. A finite element model has been developed for the rotor blade which predicts rotating frequencies quite well, across a range of rotation speeds. The helicopter is trimmed and the predicted trim-control angles are found to be in the range of measured values for a variety of flight speeds. Power predictions over a range of forward speeds also compare well. Finally, the aeroelastic analysis is used to study the importance of aerodynamic models on the vibration prediction. Unsteady aerodynamics and free-wake models have been investigated.

Keywords: Helicopter, vibration, validation, aeroelastic analysis, finite element model, rotor blade, aerodynamic models, free-wake models, unsteady aerodynamics, quasi-steady aerodynamics

NOMENCLATURE

c	Blade chord	F_{zR}	Vertical root shear force
C_T	Thrust coefficient	F	Finite element force vector
C	Finite element damping matrix	H	Shape function matrix
C_p	Main rotor power coefficient	$H(s)$	Time shape function
F_{xH}	Longitudinal hub shear force	K	Finite element stiffness matrix
F_{yH}	Lateral hub shear force	M_{xH}	Rolling hub moment
F_{zH}	Vertical hub shear force	M_{yH}	Pitching hub moment
F_{xR}	Longitudinal root shear force	M_{zH}	Yawing hub moment
F_{yR}	Lateral root shear force	M_{xR}	Rolling root moment
		M_{yR}	Pitching root moment

M_{zR}	Yawing root moment
M	Finite element mass matrix
N	Number of spatial finite elements
N_b	Number of blades
N_t	Number of time finite elements
p	Modal displacement vector
q	Global displacement vector
Q	Generalised load vector for response analysis
r	Temporal nodal displacement vector for time element
R	Rotor radius
s	Local time coordinate
T	Kinetic energy
U	Strain energy
u	Displacement vector
V	Forward speed
W	Virtual work
β_p	Blade precone
δ	Variation
Θ	Helicopter trim-control angles
Φ	Normal mode transformation matrix
ω	Frequency
μ	V / Ω_R (advance ratio)
ρ	Density of air
σ	Solidity ratio
ψ	Azimuth angle (time)
Ω	Rotation speed (scalar quantity)
Ω_R	Reference rotor speed (scalar quantity)

1. INTRODUCTION

A key tool in accelerating the helicopter design process is a comprehensive aeroelastic analysis code, which is able to simulate the behaviour of the helicopter in forward flight. These codes combine structural dynamic and aerodynamic modelling and use a physics-based approach to predict helicopter behaviour. Over the past two decades, a few such codes have been developed¹⁻³.

The objective of this study is to validate the University of Maryland Advanced Rotocraft Code (UMARC) 1.4 and understand the basic performance and vibratory effects on hingeless main rotor in forward flight. The experimental data for a 4-bladed soft-inplane hingeless main rotor has been used.

2. HELICOPTER AEROELASTIC ANALYSIS

2.1 Governing Equation of Motion

The helicopter is represented by a nonlinear model of the rotating elastic rotor blades dynamically coupled to a six-DOFs rigid fuselage. Each blade undergoes flap bending, lag bending, elastic twist, and axial displacement. Governing equation of motion derived using a generalised Hamilton's principle applicable to non-conservative systems is written as

$$\delta \Pi = \int_{\psi_1}^{\psi_2} (\delta U - \delta T - \delta W) \delta \psi \quad (1)$$

where δU , δT , and δW are the virtual strain energy, the kinetic energy, and the virtual work, respectively. The δU and δT include energy contributions from components attached to the blade, eg, pitch link, lag damper, etc. These equations are based on the work of Hodges and Dowell⁴ and include second-order geometric nonlinear terms accounting for moderate deflections in the flap bending, lag bending, and axial and torsion equations. External aerodynamic forces on the rotor blade contribute to the virtual work variation, δW .

2.1.1 Finite Element Discretisation

Finite element method is used to discretise the governing equation of motion, and it allows for accurate representation of complex hub kinematics and non-uniform blade properties. After the finite element discretisation, Hamilton's principle is written as

$$\delta \Pi = \int_0^{2\pi} \sum_{i=1}^N (\delta U_i - \delta T_i - \delta W_i) \delta \psi \quad (2)$$

Each of the N beam finite element has 15 DOFs. These DOFs correspond to cubic variations in axial elastic and flap, lag-bending deflections, and quadratic variation in elastic torsion. Between the elements, there is continuity of displacements and slope for flap and lag-bending deflections, and continuity of displacements for elastic twist and axial deflections. This element ensures physically consistent linear variations of bending moments and torsional moments and quadratic variations of axial force within the elements. The shape functions here are Hermite polynomials for lag and flap bendings and Lagrange polynomials for axial and torsional deflections. Substituting $u = H q$ (where H is the shape function matrix) in the Hamilton's principle (Eqn 2), one obtains:

$$\int_0^{2\pi} \delta q^T (M \ddot{q}(\psi) + C \dot{q}(\psi) + K q(\psi) - F(q, \dot{q}, \psi)) d\psi = 0 \quad (3)$$

The displacements, q , are functions of time and all nonlinear terms have been moved into the force vector. Spatial functionality has been removed using finite element discretisation, and partial differential equations have been converted to ordinary differential equations.

The finite element equations, representing each rotor blade, are transformed to normal mode space for efficient solution of blade using the modal expansion. The displacements are expressed in terms of normal modes as $q = \Phi p$. Substituting this equation into Eqn (3) leads to normal mode

equation having the form:

$$\int_0^{2\pi} \delta p^T (\bar{M} \ddot{p}(\psi) + \bar{C} \dot{p}(\psi) + \bar{K} p(\psi) - \bar{F}(p, \dot{p}, \psi)) d\psi = 0 \quad (4)$$

where the normal mode mass, stiffness, damping matrix, and force vector are defined as $\bar{M} = \Phi^T M \Phi$, $\bar{C} = \Phi^T C \Phi$, $\bar{K} = \Phi^T K \Phi$ and $\bar{F} = \Phi^T F$, respectively. Integrating Eqn (4) by parts, one obtains:

$$\int_0^{2\pi} \begin{Bmatrix} \delta p \\ \delta \dot{p} \end{Bmatrix} \begin{Bmatrix} \bar{F} - \bar{C} \dot{p} - \bar{K} p \\ \bar{M} \dot{p} \end{Bmatrix} d\psi = \begin{Bmatrix} \delta p \\ \delta \dot{p} \end{Bmatrix} \begin{Bmatrix} M \dot{p} \\ 0 \end{Bmatrix} \Big|_0^{2\pi} \quad (5)$$

The RHS of the Eqn. 5 is zero because of the periodicity condition of the response. Hence, Eqn (5) yields the following system of first-order differential equations:

$$\int_0^{2\pi} \delta y^T Q d\psi = 0$$

where

$$y = \begin{Bmatrix} p \\ \dot{p} \end{Bmatrix} \quad \text{and} \quad Q = \begin{Bmatrix} \bar{F} - \bar{C} \dot{p} - \bar{K} p \\ \bar{M} \dot{p} \end{Bmatrix} \quad (6)$$

2.1.2 Finite Element-Temporal Discretisation

The above equation is nonlinear because \bar{F} contains nonlinear terms. The nonlinear, periodic, ordinary differential equations are then solved for blade steady response using the finite element on time in conjunction with the Newton-Raphson method. Discretising Eqn (6) over N_t time elements around the circumference (where $\psi_1 = 0$, $\psi_{N_t+1} = 2\pi$) and taking a first-order Taylor's series expansion about the steady state value

$$y_0 = [p_0^T \dot{p}_0^T]^T$$

yields algebraic equations:

$$\sum_{i=1}^{N_t} \int_{\psi_i}^{\psi_{i+1}} \delta y_i^T Q_i(y_0 + \Delta y) d\psi$$

$$= \sum_{i=1}^{N_t} \int_{\psi_i}^{\psi_{i+1}} \delta y_i^T [Q_i(y_0 + K_{ii}(y_0)\Delta y)] d\psi = 0 \quad (7)$$

$$K_{ii} = \begin{bmatrix} \left(\frac{\partial \bar{F}}{\partial p} - \bar{K} \right) & \left(\frac{\partial \bar{F}}{\partial p} - \bar{K} \right) \\ 0 & \bar{M} \end{bmatrix} \quad (8)$$

Here, K_{ii} is the tangential stiffness matrix for time element i , and Q_i is the load vector. Also, the modal displacement vector can be written as

$$p_i(\psi) = H(s)r_i \quad (9)$$

Substituting Eqn (9) and its derivative in Eqn (7) and solving iteratively, yields the blade steady response.

2.2 Aerodynamic Modelling

2.2.1 Quasi-steady Aerodynamic Modelling

Quasi-steady aerodynamic analysis assumes that the blade air loads are solely a function of the instantaneous blade section angle of attack. The quasi-steady aerodynamic analysis results in the finite element mass, damping and stiffness matrices, and the load vector associated with the aerodynamic loading on the blade and fuselage. The calculation of this matrix requires the calculation of the incident air velocity on the blade in the deformed frame, which is given as

$$\bar{V} = -\bar{V}_w + \bar{V}_b + \bar{V}_f \quad (10)$$

where \bar{V}_w is the wind velocity with contributions from the vehicle forward speed and rotor inflow, \bar{V}_b is the blade velocity relative to the hub-fixed frame resulting from blade rotation and blade motion, and \bar{V}_f is the blade velocity due to fuselage motion. Once air velocity is calculated in the deformed plane, 2-D strip theory is used to determine the aerodynamic loads on the blade. These are written as

$$\bar{L}_e = \frac{1}{2} \rho V^2 c C_l, \quad \bar{D}_e = \frac{1}{2} \rho V^2 c C_d$$

$$\bar{M}_e = \frac{1}{2} \rho V^2 c C_m \quad (11)$$

where bar identifies forces and moments in the deformed plane, the subscript e identifies force of circulatory origin, V is the incident velocity, and C_l , C_d , and C_m are the section lift, drag, pitching moment coefficient, respectively.

2.2.2 Unsteady Aerodynamic Modelling

The aerodynamic environment is highly complex and unsteady, with regions of transonic flow, separated flow, and dynamic stall. An efficient and compatible aerodynamic model was presented by Leishman⁵. This aerodynamic model consists of an attached potential flow for linear unsteady air loads, a separated flow formulation for nonlinear unsteady air loads, and a dynamic stall formulation for vortex-induced air loads.

The attached flow formulation is based on the indicial response method, in which response is computed from a finite difference approximation to Duhamels integral. Nonlinear aerodynamic formulation for separated flow is based on Kirchhoff theory, which relates the air loads to angle of attack and the trailing edge separation point location. The dynamic stall formulation accounts for the vortex-induced aerodynamic loads. The formulation models the separation of the concentrated leading edge vortex.

2.2.3 Free-wake Aerodynamic Modelling

The main feature of this study is the use of pseudo-implicit free-wake model, which is modified to include elastic flap, lag, and torsional deformation around the azimuth⁶. The effect of the rotor cyclic controls on the blade orientation wrt the hub plane is also considered. The wake geometry is calculated in an inner loop inside the trim procedure. The blade steady response is passed on to the wake subroutines to obtain the position of the blade-control points and vortex-release points accurately. The blade flap, lag, and elastic torsional displacements

as well as rotor-control input are passed on to the wake subroutines. The wake model, however, utilises a second-order accurate accelerated-convergence pseudo-implicit iteration method that is more stable than an explicit method.

3. HUB LOADS & COUPLED TRIM

Steady and vibratory components of the non-rotating frame hub loads are calculated by the individual contributions of individual blades. For this, the motion-induced aerodynamic and inertial loads are integrated along the blade span to obtain blade loads at the roots and then summed over the blade to obtain the rotor hub loads.

$$\begin{aligned}
 F_{xH}(\psi) &= \sum_{m=1}^{N_b} (F_{xR}^m \cos\psi_m - F_{yR}^m \sin\psi_m - \beta_p F_{zR}^m \cos\psi_m) \\
 F_{yH}(\psi) &= \sum_{m=1}^{N_b} (F_{xR}^m \sin\psi_m + F_{yR}^m \cos\psi_m - \beta_p F_{zR}^m \sin\psi_m) \\
 F_{zH}(\psi) &= \sum_{m=1}^{N_b} (F_{zR}^m + \beta_p F_{xR}^m) \\
 M_{xH}(\psi) &= \sum_{m=1}^{N_b} (M_{xR}^m \cos\psi_m - M_{yR}^m \sin\psi_m \\
 &\quad - \beta_p M_{zR}^m \cos\psi_m) \\
 M_{yH}(\psi) &= \sum_{m=1}^{N_b} (M_{xR}^m \sin\psi_m + M_{yR}^m \cos\psi_m \\
 &\quad - \beta_p M_{zR}^m \sin\psi_m) \\
 M_{zH}(\psi) &= \sum_{m=1}^{N_b} (M_{zR}^m + \beta_p M_{xR}^m) \quad (12)
 \end{aligned}$$

Calculation of steady hub loads is needed to trim the helicopter. The harmonics of hub loads are responsible for vibration and dynamic stresses.

Once the hub loads are obtained, the helicopter needs to be trimmed. This is defined as the condition where the steady forces and moments acting on the helicopter sum to zero and simulates the condition

for steady-level flight. The trim solution for the helicopter involves finding the pilot control angles Θ at which the six steady forces and moments acting on the helicopter are zero:

$$F(\Theta) = 0 \quad (13)$$

The trim equations are solved iteratively using a Newton-Raphson procedure. A coupled trim procedure is carried out to solve the blade response, pilot input trim controls, and vehicle orientation, simultaneously. This procedure is called trim since the blade response [Eqns (7) and (9)] and trim [Eqn (13)] are simultaneously solved, thereby accounting for the influence of elastic blade deflections on the rotor steady forces.

$$\Delta\Theta = \left. \frac{\partial F}{\partial \Theta} \right|_{\Theta_0} (\Theta - \Theta_0), \quad \xi_{i+1}^G = \xi_i^G + \Delta\xi_i^G \quad (14)$$

The coupled trim is solved iteratively until convergence. The coupled trim procedure is essential for elastically-coupled blades since elastic deflections play an important role in the steady net forces and moments generated by the rotor.

4. HELICOPTER BASELINE MODEL

The helicopter is modelled in the University of Maryland Advanced Rotocraft Code (UMARC) as an aircraft with a single main rotor and tail rotor. The main rotor is modelled as a hingeless rotor system. Each blade is identical and is defined by undergoing flap, lead-lag, torsion, and axial degrees of motion. The blade is divided into 10 finite elements. To validate the structural model, the blade natural frequencies are calculated. Figure 1 shows the blade frequencies versus normalised rotor speed. In general, good correlation of calculated frequencies is observed with the experimental results.

To validate overall aerodynamics, the basic performance predictions at steady forward flight are compared with flight test data (Figs 2 and 3). The main rotor power predictions are plotted in Fig. 2 for nondimensional thrust coefficients C_T/σ of 0.05848 and 0.0708. Satisfactory results are obtained at all flight speeds. However, at low-flight

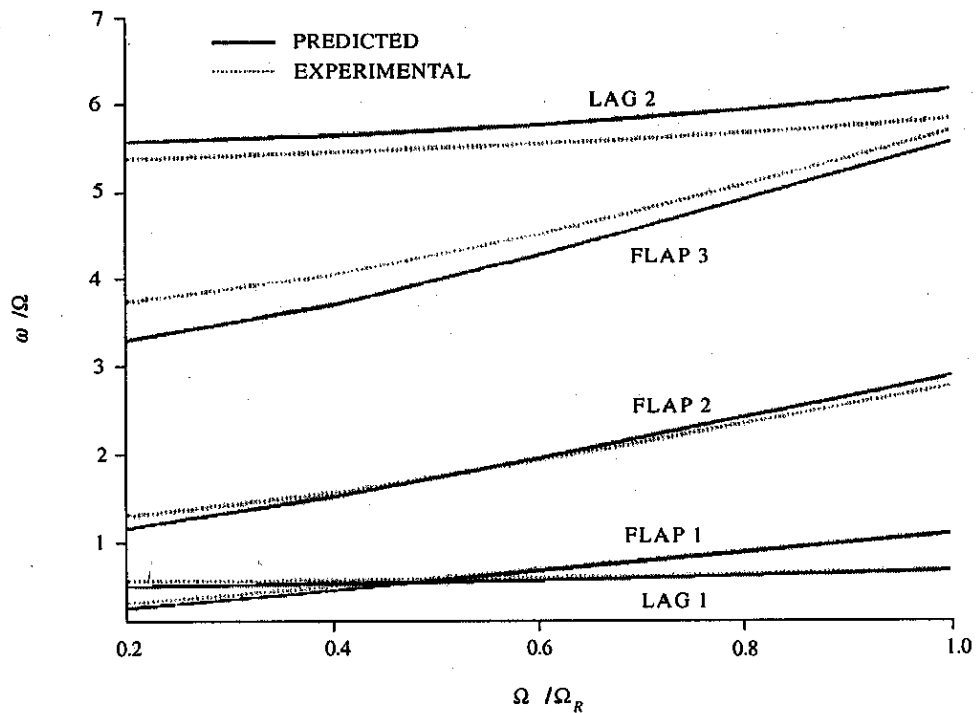


Figure 1. Hingeless main rotor blade frequencies

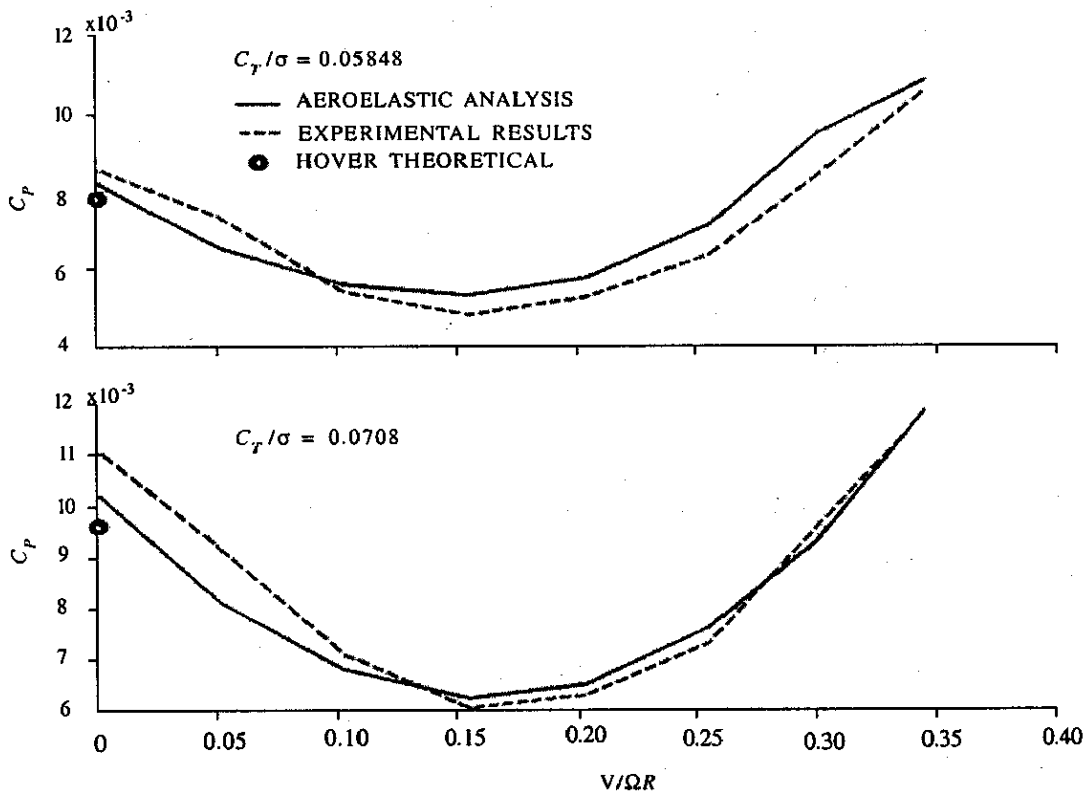


Figure 2. Nondimensional main rotor power coefficients wrt advance ratio

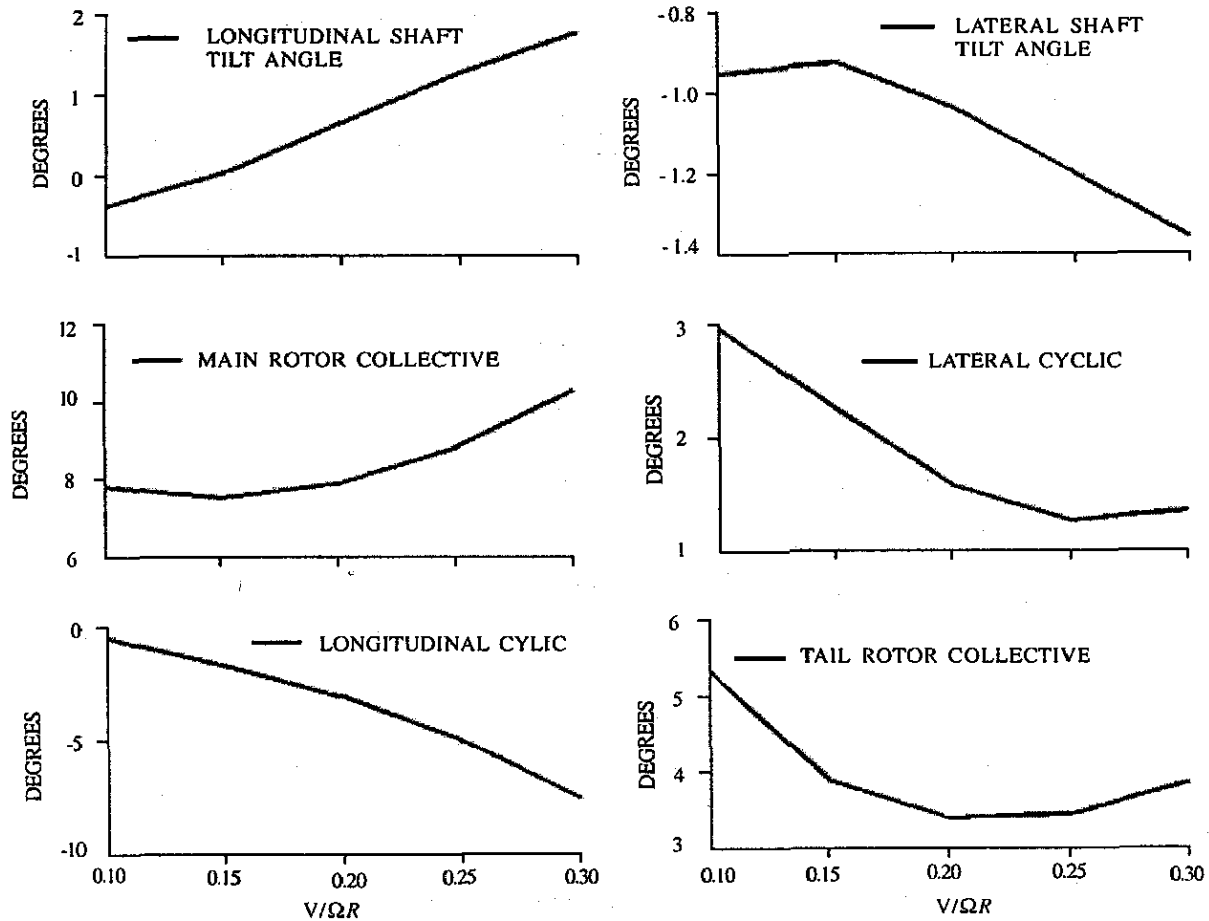


Figure 3. Trim control angles

speeds, there is slight underprediction. Figure 3 shows predicted trim control angles corresponding to $C_T/\sigma = 0.0708$, for a range of forward speeds. Predicted main rotor collective is within the specified range of -2° to 16° . Lateral cyclic and longitudinal cyclic are well within the specified ranges of -7° to 13.5° and -8° to 6° . Hence, good correlation of predicted trim control angles is observed with the experimental results.

With the basic performance and trim controls validated, the analysis was used to predict vibration. For a 4-bladed soft-inplane hingeless main rotor, the 4/rev hub loads are the main source of vibration. Figure 4 shows the predicted hub loads. The different aerodynamic effects were considered to understand the vibratory loads. Aerodynamic models used were quasi-steady and unsteady, and the inflow models used were the linear inflow and free-wake^{7,8} inflow models. The quasi-steady and unsteady aerodynamic

models results in Fig. 4 use linear inflow model and the free-wake result uses unsteady aerodynamic model. Vibratory hub loads obtained are more at hover and slowly decrease to a minimum value for low-flight speeds. But the hub loads increase during forward flight condition. The results agree with the trends in the published literature⁶, where quasi-steady aerodynamic models are known to underpredict the loads. The importance of using unsteady aerodynamic and free-wake models is highlighted.

5. CONCLUSION

A baseline model for the analysis of a soft-inplane hingeless main rotor is developed using an aeroelastic analysis code. The main rotor structural finite element model is validated by comparing frequency calculations with experimental results. The basic performance and trim angles are validated in steady forward flight. Good agreement of power

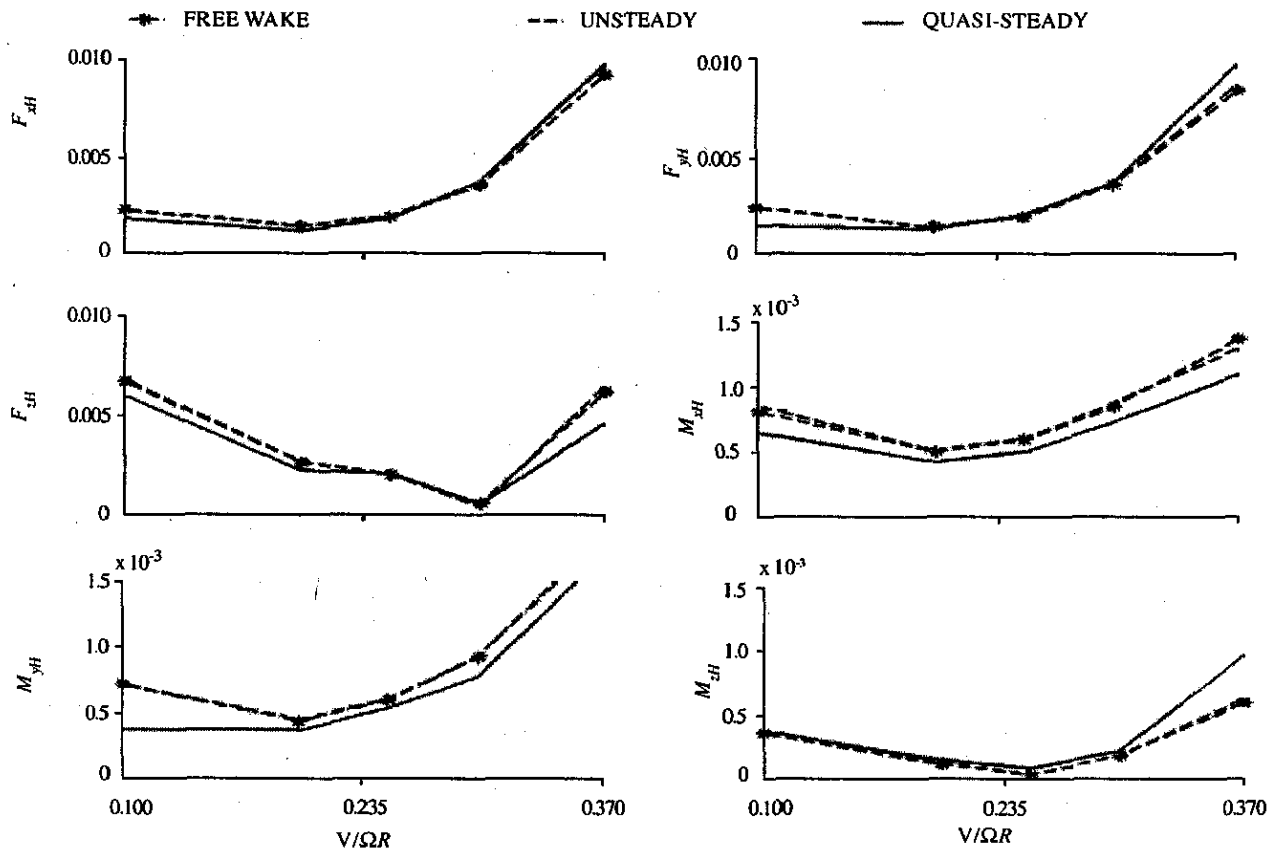


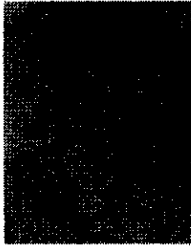
Figure 4. Amplitude of hub forces and moments

predictions with the flight test data demonstrates the validity of overall aerodynamics. The hub load calculations are performed for quasi-steady aerodynamics and unsteady inflows with linear inflows and free-wake inflow aerodynamic models.

REFERENCES

1. G. Bir, *et al.* University of Maryland advanced rotorcraft code (UMARC) theory manual. UM-AERO Report 92-02, 1992.
2. Johnson, W. A comprehensive analytical model of rotorcraft aerodynamics and dynamics, Part 1: Analysis development. National Aeronautics and Space Administration (NASA), USA. NASA Technical Memorandum No. NASA-TM-8112, June 1980.
3. Lim, J.W. Analytical investigation of UH-60A flight blade air loads and loads data. In 51st Annual Forum of the AHS. Fort Worth, Texas, May 1995.
4. Hodges, D. & Dowell, E. Nonlinear equations of motion for the elastic bending and torsion of twisted nonuniform rotor blades. National Aeronautics and Space Administration (NASA), USA. NASA Technical Note No. NASA-TN-D-7818, 1974.
5. Leishman, J.G. Indicial lift approximations for two-dimensional subsonic flow as obtained from oscillatory measurements. *Journal of Aircraft*, 1993, 30(3), 340-51.
6. Ganguli, R.; Chopra, I. & Weller, W. H. Comparison of calculated vibratory rotor hub loads with experimental data. *J. Amer. Helicopter Soc.*, 1998, 43(4), 312-18.
7. Drees, J.M. A theory of airflow through rotors and its application to some helicopter problems. *J. Helicopter Asso. Great Britain*, 1949, 3.
8. Leishman, J.G. Principles of helicopter aerodynamics. Cambridge University Press, 2000.

Contributors



Mr Shrinivas R. Bhat completed his BE (Mech Engg) from the M.S. Ramaiah Institute of Technology, Bangalore University. He is working as Research Assistant in the Dept of Aerospace Engineering, Indian Institute of Science (IISc), Bangalore.



Dr Ranjan Ganguli completed his BTech (Hons) from the Indian Institute of Technology (IIT), Kharagpur and his MS and PhD both from the University of Maryland, College Park, USA. He is working as Assistant Professor in the Dept of Aerospace Engineering, IISc, Bangalore. His areas of research include: Helicopter dynamics, health monitoring, smart structures and optimisation. He has 37 papers published in national/international journals and 20 papers published/presented in conferences.